PCCP

PAPER

View Article Online
View Journal | View Issue

Cite this: *Phys. Chem. Chem. Phys.*, 2024, **26**, 4922

Fourier-transform microwave spectroscopy of the ClSO radical†

Ching-Hua Chang, Cheng-Han Tsai, Yi-Ting Liu and Yasuki Endo *

Received 20th December 2023,
Accepted 12th January 2024

DOI: 10.1039/d3cp06185j

rsc.li/pccp

Pure rotational transitions of the ClSO radical have been observed by Fourier-transform microwave spectroscopy. a-type and b-type transitions, for both ^{35}Cl and ^{37}Cl isotopologues, were detected, and the observed very complicated fine and hyperfine components were assigned well. The intensities of the observed spectra of the two isotopologues correspond to the ratio of the isotope abundances of ^{35}Cl and ^{37}Cl. A total of 21 molecular constants were determined precisely for both ^{35}ClSO and ^{37}ClSO, including the rotational constants, centrifugal distortion constants, electronic spin-rotation constants, nuclear spin-rotation constants, magnetic hyperfine constants, and quadrupole coupling constants of chlorine. The molecular constants show ClSO to have the ^{2}A″ electronic ground state with an out-of-plane unpaired electron. The spin density of the chlorine atom is about 10.6%, which is similar to that of the fluorine atom for FSO, about 8%. Results of the ClSO radical are compared with those of other triatomic radicals with similar structures, the XSS, XSO, and XOO radicals with X = H, F, and Cl, leading to a conclusion that the ClSO radical is more like FSO, but fairly different from the FOO and ClOO radicals.

Introduction

The sulfinyl chloride radical, ClSO, has been investigated widely as it can be produced by UV absorption of thionyl chloride, Cl_2SO,[1] which is a common source of Cl atoms in organic syntheses. Cl_2SO plays an important role in chemical reactions of chlorine cycles with sulfide and other molecules in the atmosphere. It can dissociate to Cl, ClSO, Cl_2 and SO through different UV dissociation pathways,[1–3] involving:

$$Cl_2SO \rightarrow 2Cl + SO \quad \text{three-body dissociation,} \qquad (1)$$

$$Cl_2SO \rightarrow ClSO + Cl \quad \text{Cl elimination,} \qquad (2)$$

and

$$Cl_2SO \rightarrow Cl_2 + SO \quad \text{molecular elimination.} \qquad (3)$$

At 193 nm, more than 80% of Cl_2SO undergoes the three-body dissociation, and the branching ratio of the Cl-elimination channel is about 17%.[2] Only 3% of Cl_2SO dissociates through the molecular elimination. At 248 nm, the Cl-elimination channel dominates, and about 96.5% of Cl_2SO dissociates into ClSO and Cl. The remaining (3.5%) of the Cl_2SO mostly proceeds *via* the molecular elimination channel.

Cl_2SO photolysis was investigated using step-scan Fourier-transform infrared spectroscopy by Chu *et al.*[4] A mixture of Cl_2SO and Ar was photolyzed using a KrF excimer laser at 248 nm, and production of ClSO was confirmed. The S–O stretching (ν_1) mode was detected in the region 1120–1200 cm^{-1} with a resolution of 0.3 cm^{-1}. The rotational structure was revealed for the Q branch at 1162.9 cm^{-1} in the IR absorption spectrum.

More recently, an absorption spectrum in the region of 260–320 nm was detected by Chao *et al.*[5] They assigned a ClSO band around 300 nm to the $1^2A' \leftarrow X^2A''$ transition. The kinetics of the ClSO + Cl → Cl_2SO reaction was also studied using strong UV absorption at pressures in the range of 10–90 torr at 292 K.[5] They found strong pressure dependence for $k_{Cl+ClSO}$, and it was not strongly affected by the buffer gas. They also detected the absorption spectrum in the region of 350–480 nm.[6] The $1^2A' \leftarrow X^2A''$ and $2^2A' \leftarrow X^2A''$ transitions with a peak at 385 nm were observed. The conical intersection between the $1^2A'$ and $2^2A'$ excited states was calculated, and the geometry of the minimum-energy conical intersection was found to be similar to the ground-state geometry. They found that the two ^{2}A′ excited states mix due to the strong vibronic coupling.

The HSO radical, a member of a series of molecules XSO, has just been observed by Marcelino *et al.*[7] in the interstellar medium (ISM), where the fine and hyperfine components of rotational transitions of HSO were detected toward TMC-1 and the cold clouds L183, L483, L1495B, L1527, and Lupus-1A using Yebes 40 m and IRAM 30 m telescopes. This detection shows that HSO is widespread in cold dense cores. ClSO, which is a

Department of Applied Chemistry, Science Building II, National Yang Ming Chiao Tung University, 1001 Ta-Hsueh Rd., Hsinchu 300093, Taiwan. E-mail: endo@nycu.edu.tw

† Electronic supplementary information (ESI) available: Measured transition frequencies. See DOI: https://doi.org/10.1039/d3cp06185j

Table 1 Molecular constants of ^{35}ClSO determined previously and by *ab initio* calculations

	Previous work[a]	Theory[b]
A/MHz	32 819.3	32 703.9
B/MHz	4553.2	4582.5
C/MHz	3992.4	4019.3
$\|\mu_a\|$/Debye		0.59
$\|\mu_b\|$/Debye		1.83
$\|\mu_c\|$/Debye		0.00
ε_{aa}/MHz	−787.8	−818.1
ε_{bb}/MHz	−78.8	−88.3
ε_{cc}/MHz	4.4	5.2
a_F(Cl)/MHz	26.4	3.6
T_{aa}(Cl)/MHz	−19.0	−17.8
T_{bb}(Cl)/MHz	−10.9	−12.7
χ_{aa}(Cl)/MHz	−7.8	−51.5
χ_{bb}(Cl)/MHz	3.3	22.9

[a] From ref. 8. [b] Present study. The rotational constants and dipole moments were calculated at RCCSD(T)-F12/cc-pCVTZ, correlating all electrons. Other parameters were calculated at B3LYP/aug-cc-pVTZ.

chlorine substituted species of HSO, may be one of the candidates to be detected in the ISM, although the Cl abundance is not so high in the ISM.

The pure rotational spectrum of ClSO was studied by Saito *et al.* around 60 GHz using microwave spectroscopy in a glow discharge of a gas mixture of O_2 and S_2Cl_2 diluted in Ar.[8] The rotational constants, the centrifugal distortion constant Δ_N, the spin-rotation constants ε_{aa}, ε_{bb}, and ε_{cc}, and the hyperfine constants were determined in their research as given in Table 1. As the instruments being improved recent years, we could investigate this radical in more detail with Fourier transform microwave (FTMW) spectroscopy. It is also possible to study the isotopologues ^{35}ClSO and ^{37}ClSO. The FSO and HSO radicals, which also belong to the XSO molecules, have been studied using microwave and mm-wave spectroscopy,[9,10] where their fine and hyperfine constants have been determined precisely. The XSS and XOO radicals are analogous species to the XSO radicals, and that they all have the A″ ground state, and they also have been studied by rotational spectroscopy.[11–18] It is thus interesting to compare the molecular constants with these radicals to see similarities and differences.

Quantum chemical calculations

The molecular structure of ^{35}ClSO was optimized using the open-shell coupled cluster theory with perturbative triples corrections (RCCSD(T)) with explicitly correlated approximation (F12A) using the basis set of cc-pCVTZ-F12,[19,20] where all electrons were correlated. Calculations were performed using the MOLPRO 2022.3 program.[21] The rotational constants of the RCCSD(T)-F12A/cc-pCVTZ-F12 optimized structure are A_e = 32 703.8 MHz, B_e = 4582.5 MHz, and C_e = 4019.3 MHz. The values agree with those reported in ref. 8 as shown in Table 1. The calculated dipole moment component, μ_b, is much larger than μ_a. The fine and hyperfine constants were calculated using the DFT method with the B3LYP/aug-cc-pVTZ level of theory performed using the Gaussian 16 computational chemistry software package.[22] Although the DFT calculation reproduces well the spin-rotation constants and the dipolar hyperfine coupling constants, the calculated Fermi contact coupling constant and the quadrupole coupling constants are different from those reported in ref. 8.

The molecular constants of ^{37}ClSO were calculated using the same methods as those of ^{35}ClSO. Then, the rotational constants and the spin-rotation constants were scaled with the calculated values and experimentally determined values of ^{35}ClSO. The magnetic hyperfine constants and the quadrupole constants of ^{37}ClSO were calculated from the experimental values of ^{35}ClSO, which were scaled by the ratios of the magnetic moments and the quadrupole moments of ^{35}Cl and ^{37}Cl, respectively.[23]

Experimental

The pure rotational transitions of the ClSO radical were observed using a Balle-Flygare type Fourier-transform microwave (FTMW) spectrometer and a double resonance system, which have been described in detail previously.[24] In brief, the ClSO radical was generated in a supersonic jet in a pulsed-electronic discharge of a gas mixture, *ca.* 0.3% of Cl_2SO diluted in Ar or Ne. The mixture, at a stagnation pressure of typically 3 atm, was transferred to the vacuum chamber through a pulsed-solenoid valve located at the center of one of the mirrors for the Fabry–Pérot cavity. The radicals were produced by an electric discharge in the electrodes attached in front of the nozzle of the pulsed valve applying a pulsed voltage of 1.3 kV. The rotational temperature inside the cavity was below 2.5 K. Since the ClSO radical is an open-shell species, 3 Helmholtz coils surrounding the cavity were set in this study to compensate the Earth's magnetic field. The microwave pulse was emitted from an antenna located at the center of the other mirror of the cavity

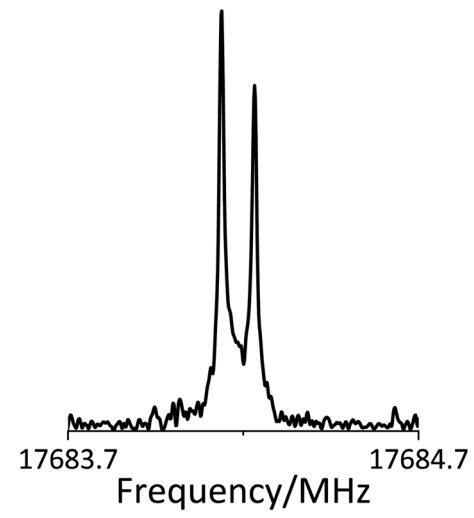

Fig. 1 FTMW spectrum of the 2_{11}–1_{10} J = 2.5–1.5 F = 2.0–1.0 transition. The spectrum is obtained by accumulating 100 shots of free induction decay signals. The spectral line shows the Doppler doubling due to the parallel orientation of the microwave and the jet propagations.

to polarize the molecules. Since the microwave pulse propagates parallel to the jet from the pulse nozzle, the spectral lines show Doppler doublings as seen in Fig. 1.

The FTMW spectrometer operates in the frequency range of 4–40 GHz to measure low-N pure rotational transitions. Transitions above 40 GHz, including the 3_{22}–4_{13}, 3_{21}–4_{14}, and 2_{21}–3_{12} transitions in the present study, were observed with an FTMW-MW double-resonance technique.[25] A microwave signal was monitored using the FTMW spectrometer, and another microwave radiation was irradiated perpendicular to the monitored microwave in the cavity as a pump microwave to measure the double-resonance signals. If a rotational transition, whose upper or lower level is shared by the monitored transition, is induced by the pump microwave, the double resonance signal is observed as a decrease of the monitor signal due to the destruction of coherence. Estimated experimental accuracies of the frequency measurements for normal FTMW experiments are about 3 kHz or less, while those of the double resonance experiments are about 10 kHz or a little bit more for weak lines when we have to put more power to observe the double resonance signals.

Results

First, b-type transitions were searched since the calculated dipole moment component μ_b is much larger than μ_a. The 3_{03}–3_{12} transition of ^{35}ClSO was expected in the region of 30 110–30 210 MHz. Four strong paramagnetic lines accompanied by weak lines were observed around 30 140 MHz, which is very close to the frequencies predicted by the *ab initio* calculations and the results in ref. 8 shown in Table 1. Then, we scanned the region from 30 350 to 30 500 to observe the other spin component. In this way, many paramagnetic lines were observed near the predicted frequencies. The observed fine and hyperfine patterns were reproduced well by the calculated fine and hyperfine constants. An example of the observed spectral pattern of the ^{35}ClSO radical is shown in Fig. 2. The upper spectrum shows the spectral lines with the Earth's magnetic field compensation, and the inverted one shows those without the compensation. The spectral lines from open-shell species disappeared or split without the compensation, showing the paramagnetic behavior. After observing b-type transitions with $K_a = 0$ and 1, we tried to observe a-type transitions. Although the dipole moment μ_a is small in the calculations, the spectral lines of 1_{01}–0_{00}, 2_{02}–1_{01}, and 3_{03}–2_{02} transitions were expected to be sufficiently strong because of the low rotational temperature inside the cavity. Later, we changed the buffer gas from Ar to Ne, since Ne is expected to have a less effective cooling effect and makes the rotational temperature higher. We tried to observe the a-type transitions with $K_a = 2$ with a sample gas, 0.3% of Cl_2SO diluted in Ne. The intensity of the 3_{22}–2_{21} transition was expected to be 11 times weaker than that of the 3_{03}–2_{02} transition when the rotational temperature is assumed to be 2.5 K. However, the actual ratio was about 30 times weaker. The rotational temperature inside the cavity may be much lower than 2.5 K, even when Ne was used as a diluent gas. We also used the mixture diluted by Ne to detect the 6_{24}–7_{17} and 7_{16}–7_{07} transitions because the energy levels of these states are relatively high.

After assigning the fine and hyperfine components of ^{35}ClSO, we tried to detect ^{37}ClSO using the scaled constants as shown in Table 3. Since the patterns of the 2_{11}–2_{02} transitions of ^{35}ClSO and ^{37}ClSO were quite similar, transitions of ^{37}ClSO were easily assigned as shown in Fig. 3. The spectral lines of ^{37}ClSO were three times weaker than those of ^{35}ClSO as expected by the population ratio of ^{35}Cl and ^{37}Cl. We used this fact to distinguish the lines of ^{37}ClSO in the complicated spectrum.

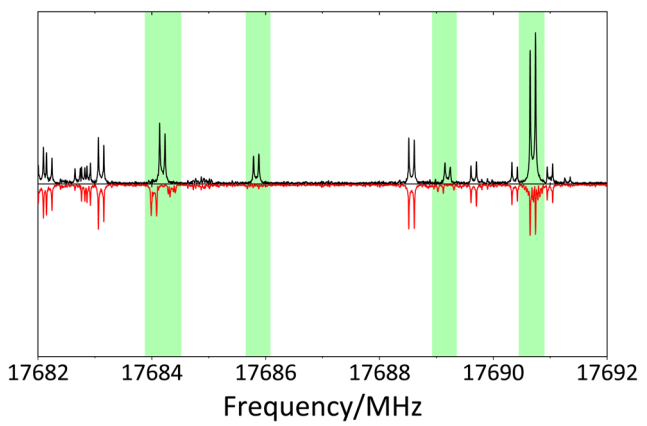

Fig. 2 Observed spectrum of ^{35}ClSO for 2_{11}–1_{10}. The upper trace (black) is that observed with the Earth's magnetic field compensation, while the lower trace (red) is that observed without the compensation. The marked spectral lines show the paramagnetic behavior, splitting or disappearance of the lines without the compensation.

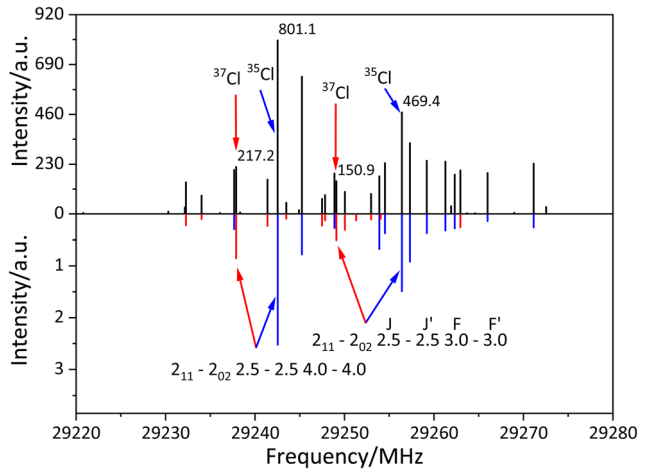

Fig. 3 Observed spectral patterns of ^{35}ClSO and ^{37}ClSO for 2_{11}–2_{02}. The upper (black) sticks are observed spectral lines, including ^{35}ClSO and ^{37}ClSO. The blue sticks are the predictions for ^{35}ClSO, and the red ones are those for ^{37}ClSO. The patterns of the two isotopologues are similar, and the intensities of the spectral lines correspond to the population ratio of ^{35}Cl and ^{37}Cl. The numbers in the spectrum are the intensities of the corresponding lines in an arbitrary unit, showing the intensity ratios between the isotopologues.

The FTMW-MW double resonance technique was applied to observe the spectral lines with transition frequencies above 40 GHz, after the fine and hyperfine components of the transitions below 40 GHz were observed. Only a small region was required to scan for observing each line since the prediction was already very accurate.

Finally, a total of 15 b-type transitions and 8 a-type transitions of ^{35}ClSO with N up to 7 and K_a = 0, 1, and 2 were observed for ^{35}ClSO. The observed transition frequencies are shown in Table S1 of the ESI.† In addition, a total of 9 b-type transitions and 6 a-type transitions with N up to 7 and K_a = 0, 1, and 2 were observed for ^{37}ClSO. The observed transition frequencies are given in Table S2 of the ESI.†

The observed transition frequencies were analyzed with the Hamiltonian,

$$\mathbf{H} = \mathbf{H}_{rot} + \mathbf{H}_{cd} + \mathbf{H}_{sr} + \mathbf{H}_{nsr} + \mathbf{H}_{hf} + \mathbf{H}_{Q}$$

where $\mathbf{H}_{rot}$ is the rotational Hamiltonian, $\mathbf{H}_{cd}$ is its centrifugal distortion term expressed in Watson's A-reduced form, $\mathbf{H}_{sr}$ is the spin-rotation term, $\mathbf{H}_{nsr}$ is the nuclear spin-rotation term, $\mathbf{H}_{hf}$ is the magnetic hyperfine term, and $\mathbf{H}_{Q}$ is the electric quadrupole coupling term. Because there is a Cl atom with nonzero nuclear spin in the radical, the following coupling scheme is adopted among the angular momenta involved

$$\mathbf{J} = \mathbf{N} + \mathbf{S},$$

and

$$\mathbf{F} = \mathbf{J} + \mathbf{I}(\mathrm{Cl}).$$

Since S = 1/2 and I(Cl) = 3/2, each rotational level splits into 8 fine and hyperfine levels.

For the ^{35}ClSO radical, the transition frequencies of the observed 244 lines were subjected to the least squares analysis using our proprietary program, where smaller weights were given for the lines measured by the double resonance method. A total of 21 molecular constants were determined with the standard deviation of the fit to be 2.3 kHz. Among the five centrifugal distortion constants, δ_K was fixed to the value obtained by the quantum chemical calculations, since it was not determinable in the fit. Similarly, for the ^{37}ClSO radical, a total of 186 spectral lines were observed, and 21 molecular constants were determined with the standard deviation of the fit to be 1.9 kHz. The determined molecular constants of the two isotopologues are given in Tables 2 and 3.

As seen in Table 2, the experimental results agree very well with those by the quantum chemical calculations. Compared to the constants given in ref. 8, the three rotational constants agree with their results with differences of 0.01%. In addition, our experimental values of the spin-rotation constants and the magnetic dipolar coupling constants agree with their values with differences of about 10% or even less. However, the experimental results for the Fermi contact coupling constant and the quadrupole coupling constants are quite different from their values.

Table 2 Molecular constants of ^{35}ClSO[ab] (in MHz)

	Exp.	Theory[c]
A	32 823.64409(37)	32 703.9
B	4553.94358(11)	4582.5
C	3992.35645(10)	4019.3
$\Delta_N/10^{-3}$	2.6054(20)	2.6
$\Delta_{NK}/10^{-3}$	−21.832(23)	−21.2
$\Delta_K/10^{-3}$	599.554(93)	573.0
$\delta_N/10^{-3}$	0.47257(93)	0.45
$\delta_K/10^{-3}$	14.0[d]	14.0
ε_{aa}	−779.83736(79)	−818.1
ε_{bb}	−85.56951(29)	−88.3
ε_{cc}	3.54021(34)	5.2
ε_{ab}	−36.0827(93)	−26.8
a_F(Cl)	3.23324(37)	3.6
T_{aa}(Cl)	−17.33846(63)	−17.8
T_{bb}(Cl)	−11.74443(58)	−12.7
T_{ab}(Cl)	3.060(29)	1.25
χ_{aa}(Cl)	−51.9147(15)	−51.5
χ_{bb}(Cl)	22.3736(16)	22.9
χ_{ab}(Cl)	26.02(16)	25.6
C_{aa}(Cl)	0.00670(36)	0.0070
C_{bb}(Cl)	0.00229(12)	0.0025
C_{ab}(Cl)	0.00262(14)	0.0026

[a] Values in parentheses are 1σ errors applied to the last digits of the parameters. [b] Standard deviation of the fit is 2.3 kHz. [c] The rotational constants were calculated at RCCSD(T)-F12/cc-pCVTZ, correlating all electrons. Other parameters were calculated at B3LYP/aug-cc-pVTZ. [d] The value without uncertainty is kept fixed to that obtained theoretically.

Table 3 Molecular constants of ^{37}ClSO[ab] (in MHz)

	Exp.	Scaled[c]
A	32 713.93290(48)	32 676.9
B	4422.36640(16)	4420.1
C	3889.73021(21)	3887.3
$\Delta_N/10^{-3}$	2.4706(45)	2.4
$\Delta_{NK}/10^{-3}$	−20.944(53)	−20.9
$\Delta_K/10^{-3}$	593.00(13)	593.0
$\delta_N/10^{-3}$	0.4366(47)	0.4
$\delta_K/10^{-3}$	13.5[e]	13.5
ε_{aa}	−777.00024(71)	−773.0
ε_{bb}	−83.24599(28)	−83.6
ε_{cc}	3.44907(42)	3.5
ε_{ab}	−35.2860(93)	−36.0
a_F(Cl)[d]	2.69324(39)	2.7
T_{aa}(Cl)	−14.44729(59)	−14.4
T_{bb}(Cl)	−9.76197(62)	−9.8
T_{ab}(Cl)	2.515(25)	2.6
χ_{aa}(Cl)[e]	−41.0592(14)	−40.9
χ_{bb}(Cl)	17.7810(15)	17.6
χ_{ab}(Cl)	20.38(15)	20.6
C_{aa}(Cl)	0.00610(36)	0.0058
C_{bb}(Cl)	0.00160(13)	0.0020
C_{ab}(Cl)	0.00217(15)	0.0021

[a] Values in parentheses are 1σ errors applied to the last digits of the parameters. [b] Standard deviation of the fit is 1.9 kHz. [c] The parameters were calculated using the same methods for ^{35}ClSO, and they were scaled with the experimental values for ^{35}ClSO. [d] The scaled hyperfine constants and the quadrupole coupling constants are calculated using the ratios of the magnetic moments and quadrupole moments of the two isotopes, respectively. [e] The value without uncertainty is kept fixed to that obtained theoretically.

Discussion

The molecular constants of ClSO show characteristic features of the radical, especially for the unpaired electron. The negative

value of the electron spin-rotation constant ε_{aa} indicates that the unpaired electron occupies the π-orbital perpendicular to the molecular plane, or the radical has the $^2A''$ ground electronic state. Table 4 compares the rotational constants and the spin-rotation constants for related radicals, XSO, XSS, and XOO, where X = H, F, and Cl. All of them listed here have negative ε_{aa}, and are considered to have the $^2A''$ ground electronic state. Most of the radicals in Table 4 have very small ε_{cc} values, except for FOO and ClOO, which are also the characteristic for triatomic radicals with the $^2A''$ ground states.

The positive value of a_F is mainly attributed to the spin polarization effect of the Cl–S σ-bonding orbital due to the unpaired π-electron on the chlorine atom. Moreover, since the F–S bond is shorter than the Cl–S bond and the magnetic moment of the F atom is larger than that of the Cl atom, a_F of FSO has a much larger value. On the other hand, for the XOO radicals (X = F or Cl), the unpaired electron orbital retains the π* nature of the O_2 molecule, leading to much longer and weaker X–O bonds than those of other species, and the Fermi contact constants a_F of the XOO radicals have negative values. In the case of the HSO, HSS and HOO radicals, there is no spin density on the hydrogen atoms, and the negative values of a_F are due to the spin-polarization of the H–S or H–O σ-bond due to the unpaired electron density on the neighboring S/O atom.

The calculated unpaired electron orbital of ClSO is shown in Fig. 4 along with its principal axes. Since $T_{aa} + T_{bb} + T_{cc} = 0$, T_{cc} is calculated to be 29.1 MHz for ^{35}ClSO. From this value, the spin density on the chlorine p_c orbital is estimated to be about 10.6%,[27] which is slightly larger than the spin density on the fluorine p_c orbital of FSO, about 8%.[9] In principle, the relationship, $T_{cc} \cong -2\ T_{aa} \cong -2\ T_{bb}$, is satisfied for the magnetic dipolar constants for species with an unpaired electron in an out-of-plane p_c orbital of the nucleus. The dipolar coupling constants of the related radicals are given in Table 5. Similar to FSO, the ClSO radical roughly follows this rule, while it is not satisfied for XOO radicals since the unpaired electron on the XOO radical is almost confined to the O_2 part.

The rotation angle from the *a*-axis to the *x*-axis is about 23.8°, as shown in Table 6, where *x*, *y*, and *z* are the principal axes of the magnetic dipolar interaction tensor, where the *z*-axis is identical to the *c*-axis. It is larger than the angle between the Cl–S bond and the *a*-axis which is calculated to be 17.8°. It is difficult to explain the difference, since the unpaired electron on the oxygen atom also contributes to the tensor. The principal axis values of the quadrupole coupling tensor are also given in Table 6. In this case, the rotation angle from the *a*-axis to the *x*-axis is 17.5°, which clearly shows that the principal axis *x* of the quadrupole coupling tensor is almost parallel to the Cl–S bond and their components are axially symmetric. The value of the quadrupole coupling constant χ_{xx} along the Cl–S axis, −60.1 MHz, indicates that the Cl–S bond has a character between the ionic and the covalent characters.[26]

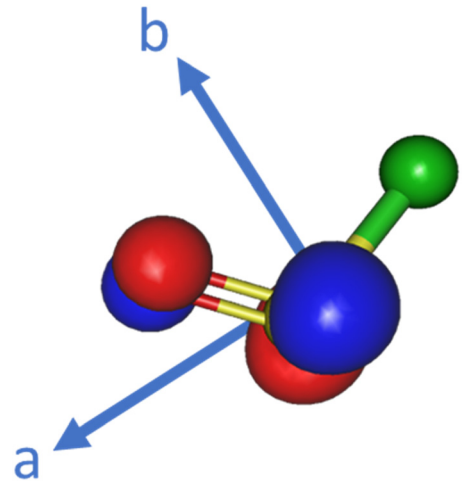

Fig. 4 Figure of the ClSO radical showing the principal axes (a and b) and the unpaired electron orbital, where the green ball is the chlorine atom.

Table 5 Magnetic hyperfine coupling constants of ClSO and other radicals (in MHz)

	a_F	T_{aa}	T_{bb}	T_{cc}	$\lvert T_{ab}\rvert^i$
ClSO[a]	3.23	−17.33	−11.74	29.07	3.06
HSO[b]	−36.37	−11.96	10.44	1.52	−7.8
FSO[c]	67.23	−118.16	−117.06	235.12	10.29
HSS[d]	−22.42	−5.87	5.84	0.03	−4.20
FSS[e]	44.17	−75.14	−74.50	149.64	16.61
HOO[f]	−27.48	−8.34	19.68	−11.34	−18.3
FOO[g]	−33.87	−212.86	9.31	203.55	139.18
ClOO[h]	−11.17	−38.87	11.51	27.36	16.62

[a] Present study. [b] From ref. 10. [c] From ref. 9. [d] From ref. 17. [e] From ref. 12. [f] From ref. 13. [g] From ref. 16. [h] From ref. 14. [i] The relative signs correspond to ε_{ab}.

Table 4 Rotational constants and spin-rotation constants of ClSO and other similar triatomic radicals (in MHz)

	A	*B*	*C*	ε_{aa}	ε_{bb}	ε_{cc}	ε_{ab}
ClSO[a]	32 823.64	4553.94	3992.36	−779.84	−85.57	3.54	−36.08
HSO[b]	299 484.63	20 504.56	19 133.93	−10 365.99	−426.66	0.23	378.0
FSO[c]	38 698.18	9340.81	7505.06	−339.54	34.90	1.86	207.95
HSS[d]	296 978.96	7996.37	7776.74	−45 926.76	−424.36	10.07	234.70
FSS[e]	26 563.82	4864.68	4103.89	−742.18	−148.29	2.70	260.56
ClSS[f]	18 319.80	2827.55	2445.93	−1329.1	−121.29	1.73	17.9
HOO[g]	61 0273.22	33 517.82	31 667.65	−49 571.41	−422.76	8.61	0.39
FOO[h]	78 430.14	10 013.94	8855.25	−887.60	−47.96	20.85	69.31
ClOO[i]	74 541.99	4936.73	4621.17	−1325.69	17.31	113.37	−38.2

[a] Present study. [b] From ref. 10. [c] From ref. 9. [d] From ref. 17. [e] From ref. 12. [f] From ref. 11. [g] From ref. 15. [h] From ref. 16. [i] From ref. 14.

Table 6 Principal axis values of T and χ tensors (in MHz)

	^{35}ClSO	^{37}ClSO
a_F(Cl)	3.23	2.69
θ_T[a]/deg.	23.8	24.3
T_{xx}(Cl)	−18.69	−15.54
T_{yy}(Cl)	−10.40	−8.67
T_{zz}(Cl)	29.09	24.21
θ_χ[b]/deg.	17.5	17.6
χ_{xx}(Cl)	−60.12	−47.43
χ_{yy}(Cl)	30.58	24.15
χ_{zz}(Cl)	29.54	23.28

[a] The rotation angle from the a-axis to the x-axis, in degree. [b] The rotation angle from the a-axis to the x-axis, in degree.

Table 7 Molecular structures of ClSO and other related molecules

	r(X–S or X–O)/Å	r(S–S, S–O or O–O)/Å	∠(XSS, XSO or XOO)/deg.
ClSO[a]	2.052	1.463	109.86
FSO[b]	1.602	1.452	108.32
SO[c]		1.481	
SO_2[d]		1.431	
SF[e]	1.587		
HSS[f]	1.364	1.965	101.7
FSS[g]	1.595	1.915	107.8
ClSS[h]	2.071	1.906	110.3
S_2[i]		1.889	
S_3[j]		1.917	
HOO[k]	0.972	1.329	104.5
FOO[l]	1.649	1.200	111.2
ClOO[m]	2.084	1.207	115.4
O_2[n]		1.208	
ClO[o]	1.570		

[a] Present study. [b] From ref. 9. [c] From ref. 28. [d] From ref. 32. [e] From ref. 33. [f] From ref. 17. [g] From ref. 12. [h] From ref. 11. [i] From ref. 29. [j] From ref. 30. [k] From ref. 15. [l] From ref. 16. [m] From ref. 18. [n] From ref. 31. [o] From ref. 34.

The r_0 structure of ClSO was determined from the moments of inertia for the two isotopologues. The determined structural parameters are compared with those of related molecules in Table 7. The S–O bond lengths of FSO and ClSO are shorter than that of SO.[28] For the XSS radicals, they still follow this tendency.[11,12] Furthermore, the S–S bond lengths of the FSS and ClSS radicals are between those of the S_2 and S_3 molecules.[29,30] On the other hand, the O–O bond lengths of the XOO (X = F or Cl) radicals are almost the same as that of the O_2 molecule.[31] This fact indicates that the O_2 part of the XOO radicals retain the character of the O_2 molecule.

Conclusions

Pure rotational transitions of both the ^{35}Cl and ^{37}Cl isotopologues were observed by FTMW spectroscopy, and the observed fine and hyperfine components for each rotational transition were assigned well. The molecular constants including the fine and hyperfine coupling constants are determined precisely in this study. We compared the determined constants of ClSO to those of a number of triatomic radicals with same symmetry and similar structures. ClSO is found to be similar to FSO, but fairly different from FOO and ClOO. Since HSO has just been detected by Marcelino *et al.* in interstellar space[7] and the formation of the ClSO radical has been studied extensively, the present data could be facilitated for the detection of atmospheric or interstellar ClSO.

Author contributions

Ching-Hua Chang: data curation, formal analysis, investigation, and writing – review and editing. Cheng-Hua Tsai: formal analysis and investigation. Yi-Ting Liu: formal analysis and investigation. Yasuki Endo: conceptualization, data curation, formal analysis, funding acquisition, methodology, software, and writing – review and editing.

Conflicts of interest

There are no conflicts to declare.

Acknowledgements

This work was supported by the Ministry of Science and Technology, Taiwan (grants MOST108-2113-M-009-025 and MOST109-2113-M-009-024).

References

1 A. P. Uthman, P. J. Demlein, T. D. Allston, M. C. Withiam, M. J. McClements and G. A. Takacs, Photoabsorption spectra of gaseous methyl bromide, ethylene dibromide, nitrosyl bromide, thionyl chloride, and sulfuryl chloride, *J. Phys. Chem.*, 1978, **82**, 2252–2257.
2 H. Wang, X. Chen and B. R. Weiner, Laser photodissociation dynamics of thionyl chloride: concerted and stepwise cleavage of S-Cl bonds, *J. Phys. Chem.*, 1993, **97**, 12260–12268.
3 G. Baum, C. Effenhauser, P. Felder and J. Huber, Photofragmentation of thionyl chloride: Competition between radical, molecular, and three-body dissociations, *J. Phys. Chem.*, 1992, **96**, 756–764.
4 L.-K. Chu, Y.-P. Lee and E. Y. Jiang, Detection of ClSO with time-resolved Fourier-transform infrared absorption spectroscopy, *J. Chem. Phys.*, 2004, **120**, 3179–3184.
5 W. Chao, G. H. Jones, M. Okumura, C. J. Percival and F. A. F. Winiberg, Spectroscopic and Kinetic Studies of the ClSO Radical from Cl_2SO Photolysis, *J. Am. Chem. Soc.*, 2022, **144**, 20323–20331.
6 W. Chao, G. H. Jones, M. Okumura, C. J. Percival and F. A. F. Winiberg, A-Band Absorption Spectrum of the ClSO Radical: Electronic Structure of the Sulfinyl Group, *J. Phys. Chem. A*, 2023, **127**, 8374–8382.
7 N. Marcelino, C. Puzzarini, M. Agúndez, R. Fuentetaja, B. Tercero, P. de Vicente and J. Cernicharo, First detection of the HSO radical in space, *Astron. Astrophys.*, 2023, **674**, L13.

8 S. Saito, Y. Endo and E. Hirota, presented in part at the General Discussion on Molecular Structure, Fukuoka, 1980.
9 Y. Endo, S. Saito and E. Hirota, Microwave spectrum, spin–rotation, and hyperfine interaction constants, dipole moment, molecular structure, and harmonic force constants of the FSO radical, *J. Chem. Phys.*, 1981, **74**, 1568–1579.
10 Y. Endo, S. Saito and E. Hirota, Microwave spectra of the HSO and DSO radicals, *J. Chem. Phys.*, 1981, **75**, 4379–4384.
11 M. Fujitake and E. Hirota, The microwave spectrum of the ClS_2 free radical, *Can. J. Phys.*, 1994, **72**, 1043–1050.
12 J. Tang and S. Saito, Microwave spectrum of the FS_2 radical in the ground electronic $\tilde{X}\,^2A''$ state, *J. Chem. Phys.*, 1996, **104**, 7437–7443.
13 C. E. Barnes, J. M. Brown, A. Carrington, J. Pinkstone, T. J. Sears and P. J. Thistlethwaite, The EPR spectrum of the HO_2 radical and determination of ground state parameters, *J. Mol. Spectrosc.*, 1978, **72**, 86–101.
14 K. Suma, Y. Sumiyoshi and Y. Endo, Fourier transform microwave spectroscopy and Fourier transform microwave–millimeter wave double resonance spectroscopy of the ClOO radical, *J. Chem. Phys.*, 2004, **121**, 8351–8359.
15 A. Charo and F. C. De Lucia, The millimeter and submillimeter spectrum of HO2: The effects of unpaired electronic spin in a light asymmetric rotor, *J. Mol. Spectrosc.*, 1982, **94**, 426–436.
16 M. Bogey, P. B. Davies, C. Demuynck, J. L. Destombes and T. J. Sears, The microwave spectrum of the FO_2 radical, *Mol. Phys.*, 1989, **67**, 1033–1051.
17 M. Tanimoto, T. Klaus, H. S. P. Müller and G. Winnewisser, Rotational Spectra of the Thiosulfeno Radical, HSS and DSS, between 0.3 and 0.9 THz, *J. Mol. Spectrosc.*, 2000, **199**, 73–80.
18 H. Uehara, K. Kawaguchi and E. Hirota, Diode laser spectroscopy of the $\nu 3$ and $\nu 2$ fundamental bands of DO_2, *J. Chem. Phys.*, 1985, **83**, 5479–5485.
19 G. Knizia, T. B. Adler and H. J. Werner, Simplified CCSD(T)-F12 methods: theory and benchmarks, *J. Chem. Phys.*, 2009, **130**, 054104.
20 J. G. Hill, S. Mazumder and K. A. Peterson, Correlation consistent basis sets for molecular core-valence effects with explicitly correlated wave functions: The atoms B–Ne and Al–Ar, *J. Chem. Phys.*, 2010, **132**, 054108.
21 H.-J. Werner, P. J. Knowles, G. Knizia, F. R. Manby, M. Schütz, P. Celani, W. Györffy, D. Kats, T. Korona, R. Lindh, A. Mitrushenkov, G. Rauhut, K. R. Shamasundar, T. B. Adler, R. D. Amos, S. J. Bennie, A. Bernhardsson, A. Berning, D. L. Cooper, M. J. O. Deegan, A. J. Dobbyn, F. Eckert, E. Goll, C. Hampel, A. Hesselmann, G. Hetzer, T. Hrenar, G. Jansen, C. Köppl, S. J. R. Lee, Y. Liu, A. W. Lloyd, Q. Ma, R. A. Mata, A. J. May, S. J. McNicholas, W. Meyer, T. F. Miller III, M. E. Mura, A. Nicklass, D. P. O'Neill, P. Palmieri, D. Peng, K. Pflüger, R. Pitzer, M. Reiher, T. Shiozaki, H. Stoll, A. J. Stone, R. Tarroni, T. Thorsteinsson, M. Wang and M. Welborn, *MOLPRO, version 2022.1*, a package of ab initio programs, 2022, see **https://www.molpro.net**.
22 M. J. Frisch, G. W. Trucks, H. B. Schlegel, G. E. Scuseria, M. A. Robb, J. R. Cheeseman, G. Scalmani, V. Barone, G. A. Petersson, H. Nakatsuji, X. Li, M. Caricato, A. V. Marenich, J. Bloino, B. G. Janesko, R. Gomperts, B. Mennucci, H. P. Hratchian, J. V. Ortiz, A. F. Izmaylov, J. L. Sonnenberg, D. Williams-Young, F. Ding, F. Lipparini, F. Egidi, J. Goings, B. Peng, A. Petrone, T. Henderson, D. Ranasinghe, V. G. Zakrzewski, J. Gao, N. Rega, G. Zheng, W. Liang, M. Hada, M. Ehara, K. Toyota, R. Fukuda, J. Hasegawa, M. Ishida, T. Nakajima, Y. Honda, O. Kitao, H. Nakai, T. Vreven, K. Throssell, J. A. Montgomery Jr., J. E. Peralta, F. Ogliaro, M. J. Bearpark, J. J. Heyd, E. N. Brothers, K. N. Kudin, V. N. Staroverov, T. A. Keith, R. Kobayashi, J. Normand, K. Raghavachari, A. P. Rendell, J. C. Burant, S. S. Iyengar, J. Tomasi, M. Cossi, J. M. Millam, M. Klene, C. Adamo, R. Cammi, J. W. Ochterski, R. L. Martin, K. Morokuma, O. Farkas, J. B. Foresman and D. J. Fox, *CT2016*, Gaussian, Wallingford.
23 N. J. Stone, Table of nuclear magnetic dipole and electric quadrupole moments, *At. Data Nucl. Data Tables*, 2005, **90**, 75–176.
24 C. Cabezas, J.-C. Guillemin and Y. Endo, Fourier-transform microwave spectroscopy of a halogen substituted Criegee intermediate ClCHOO, *J. Chem. Phys.*, 2016, **145**, 184304.
25 Y. Sumiyoshi, H. Katsunuma, K. Suma and Y. Endo, Spectroscopy of Ar–SH and Ar–SD. I. Observation of rotation-vibration transitions of a van der Waals mode by double-resonance spectroscopy, *J. Chem. Phys.*, 2005, **123**, 054324.
26 W. Gordy, in *Microwave Molecular Spectra*, ed. R. L. Cook, Wiley, New York, 3rd edn, 1984.
27 J. R. Morton, Electron Spin Resonance Spectra of Oriented Radicals, *Chem. Rev.*, 1964, **64**, 453–471.
28 K. Kawaguchi, C. Yamada and E. Hirota, Laser magnetic resonance spectroscopy of SO in the $X\,3\Sigma-$ state with a CO_2 laser as a source, *J. Chem. Phys.*, 1979, **71**, 3338–3345.
29 E. H. Fink, H. Kruse and D. A. Ramsay, The high-resolution emission spectrum of S2 in the near infrared: The $b^1\Sigma g +$ -$X^3\Sigma g-$ system, *J. Mol. Spectrosc.*, 1986, **119**, 377–387.
30 M. C. McCarthy, S. Thorwirth, C. A. Gottlieb and P. Thaddeus, The Rotational Spectrum and Geometrical Structure of Thiozone, S3, *J. Am. Chem. Soc.*, 2004, **126**, 4096–4097.
31 K. P. Huber and G. Herzberg, *Molecular Spectra and Molecular Structure IV. Constants of Diatomic Molecules*, Van Nostrand Reinhold, New York, 1979.
32 S. Saito, Microwave spectrum of sulfur dioxide in doubly excited vibrational states and determination of the γ constants, *J. Mol. Spectrosc.*, 1969, **30**, 1–16.
33 T. Amano and E. Hirota, Microwave spectrum of the SF radical, *J. Mol. Spectrosc.*, 1973, **45**, 417–419.
34 T. Amano, S. Saito, E. Hirota, Y. Morino, D. R. Johnson and F. X. Powell, Microwave spectrum of the ClO radical, *J. Mol. Spectrosc.*, 1969, **30**, 275–289.

